# Singlet and Triplet Biradical Intermediates in the Valence Isomerization of 2,7-Dihydro-2,2,7,7-tetramethylpyrene

**Erich Hasler, Aldo Hörmann, Gabriele Persy, Herbert Platsch, and Jakob Wirz***

*Contribution from the Institut für Physikalische Chemie der Universität Basel, Klingelbergstrasse 80, CH-4056 Basel, Switzerland*

*Received December 3, 1992*

**Abstract:** The photochemical and thermal reaction paths in the valence isomerization 2,7-dihydro-2,2,7,7-tetramethylpyrene (**1**) ⇄ 2,2,7,7-tetramethyldicyclopropa[*a*,*g*]pyracene (**2**) were traced by flash photolysis, optical and ESR spectroscopy, thermal reaction kinetics, and oxygen trapping experiments. The heat evolved in the reaction **2** → **1** was determined by differential scanning and photoacoustic calorimetry. All reactions connecting **1** and the two geometric isomers of **2** proceed through a common perinaphthadiyl biradical intermediate (**b**, Scheme I). State-symmetry correlation proved to be a valuable guideline to excited-state reactivity. Singlet biradical $^1$**b**, which forms with unit quantum yield upon irradiation of either **1** or **2**, was observed by picosecond pump–probe flash photolysis ($\tau$ = 18 ps). The predominant decay channel of $^1$**b** is cyclization yielding **2**. Hence, the quantum yield of the photochemical valence isomerization **1** ⇄ **2** is near unity in the forward direction and only 5% in the backward direction. The ground state of the biradical is a triplet state, $^3$**b**, but intersystem crossing (ISC) is negligible in thermal and photochemical isomerization reactions at or above room temperature. Entry to the triplet manifold is provided by triplet sensitization, by oxygen-catalyzed ISC, or by direct irradiation of **2** at low temperature. At room temperature, $^3$**b** is long-lived, $\tau$ = 660 $\mu$s, and readily trapped by molecular oxygen, $k = 1.3 \times 10^9$ M$^{-1}$ s$^{-1}$. At 77 K, $^3$**b** is persistent and photoisomerization requires two photons, the second for excitation of intermediate $^3$**b**. The adiabatic ring opening $^3$**2** → $^3$**b** occurs exclusively from an upper triplet state of **2**, as predicted by state-symmetry analysis.

In 1962, Doering and Roth coined the expression "no-mechanism reactions" to designate "thermo-reorganization reactions ... which in modern mechanistic scrutiny disclose insensitivity to catalysis, little response to changes in medium and no involvement of common intermediates ...".[1] The Woodward–Hoffmann rules have since brought an important theoretical classification that attributes a concerted (single-step) pathway to the preferred "allowed" reactions and relegates the occurrence of biradical intermediates to either enforced "forbidden" or photochemical reactions.[2] In contrast to the wealth of information available on triplet biradical intermediates, little is known about the properties of singlet biradicals that may be involved in valence isomerization reactions, and it is an open question whether intersystem crossing (ISC) to the triplet manifold is of importance at biradicaloid geometries. The goal of this work was to identify thermal and photochemical pathways and reaction intermediates in valence isomerization of a hydrocarbon.

In a preliminary communication, we reported the synthesis of 2,7-dihydro-2,2,7,7-tetramethylpyrene (**1**) and its photochemical, thermoreversible valence isomerization to the two geometrical isomers 2,2,7,7-tetramethyldicyclopropa[*a*,*g*]pyracene[3] (*syn*-**2** and *anti*-**2**).[4] The methyl groups serve to protect dihydropyrene **1** against tautomerization, disproportionation, and oxidation. Geometrical constraints force the pericyclic reaction **1** ⇄ **2** to follow a [$6_s + 6_s$], ground-state-forbidden[2] pathway. Hence, the ground-state reaction should occur in a stepwise fashion through a perinaphthadiyl biradical intermediate (**b**). Related non-Kekulé hydrocarbons (1,8-naphthoquinodimethanes) are extensively characterized in their triplet ground state both as transient intermediates in solution and as persistent species at low temperature.[5] Therefore, we chose the system **1** ⇄ **2** as a model to study the role of biradical intermediates in a valence isomerization reaction.

**Scheme I**

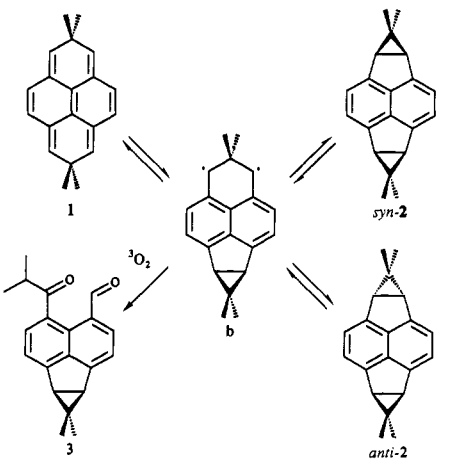


## Results

**Semiempirical Calculations.** The singlet excitation energies and transition moments of **1** were calculated by the PPP SCF CI

(1) Doering, W. v. E.; Roth, W. R. *Tetrahedron* **1962**, *18*, 67.

(2) Woodward, R. B.; Hoffmann, R. *Angew. Chem.* **1969**, *81*, 797; *Angew. Chem., Int. Ed. Engl.* **1969**, *8*, 781. For challenges for this simple rule, cf. Dewar, M. J. S.; Jie, C. *Acc. Chem. Res.* **1992**, *25*, 537.

(3) IUPAC nomenclature, *syn*-**2**: (1a$\alpha$,3b$\alpha$,4a$\alpha$,6b$\alpha$)-1,1a,3b,4,4a,6b-hexahydro-1,1,4,4-tetramethylcyclopropa[*a*]cyclopropa[4,5]cyclopent[1,2,3-*fg*]acenaphthylene. *anti*-**2**: (1a$\alpha$,3b$\beta$,4a$\beta$,6b$\alpha$)-1,1a,3b,4,4a,6b-hexahydro-1,1,4,4-tetramethylcyclopropa[*a*]cyclopropa[4,5]cyclopent[1,2,3-*fg*]-acenaphthylene.

(4) Ackermann, J.; Angliker, H.; Hasler, E.; Wirz, J. *Angew. Chem.* **1982**, *94*, 632; Angew. *Chem., Int. Ed. Engl.* **1982**, *21*, 618; *Angew. Chem., Suppl.* **1982**, 1429.

(5) (a) Pagni, R. M.; Burnett, M. N.; Dodd, J. R. *J. Am. Chem. Soc.* **1977**, *99*, 1972. (b) Muller, J.-F.; Muller, D.; Dewey, H. J.; Michl, J. *Ibid.* **1978**, *100*, 1629. (c) Gisin, M.; Rommel, E.; Wirz, J.; Burnett, M. N.; Pagni, R. M. *Ibid.* **1979**, *101*, 2216. (d) Platz, M. S. *Ibid.* **1979**, *101*, 3398. (e) Platz, M. S.; Burns, J. R. *Ibid.* **1979**, *101*, 4425. (f) Platz, M. S. *Ibid.* **1980**, *102*, 1192. (g) Hasler, E.; Gassmann, E.; Wirz, J. *Helv. Chim. Acta* **1985**, *68*, 777. (h) Fischer, J. J.; Penn, J. H.; Döhnert, D.; Michl, J. *J. Am. Chem. Soc.* **1986**, *108*, 1715. (i) Fischer, J. J.; Michl, J. *Ibid.* **1987**, *109*, 583. (j) Burnett, M. N.; Boothe, R.; Clark, E.; Gisin, M.; Hassaneen, H. M.; Pagni, R. M.; Persy, G.; Smith, R. J.; Wirz, J. *Ibid.* **1988**, *110*, 2527. (k) Biewer, M. C.; Platz, M. S.; Roth, M.; Wirz, J. *Ibid.* **1991**, *113*, 8069.

0002-7863/93/1515-5400$04.00/0 

**Table I.** Experimental and Calculated (PPP SCF CI) Singlet Absorption Bands of **1**; Symmetry Labels ($D_{2h}$) Refer to *y* and *z* in the Plane of the $\pi$-System, *z* Parallel to Double Bonds

| state sym | λ/nm | osc strength (*f*) calcd | polarization | $\lambda_{0-0}$/nm (log ε) obsd |
|---|---|---|---|---|
| | | Singlet–Singlet ($S_0 - S_x$) Transitions | | |
| $B_{3g}$ | 436 | 0 | | 415 sh (3.4) |
| $B_{1u}$ | 433 | 0.27 | | 379 (4.38) |
| $B_{3g}$ | 352 | 0 | | |
| $B_{1u}$ | 294 | 0 | parity forbidden | 315 (3.7) |
| $B_{1u}$ | 286 | 0.44 | *z* | 271 (4.91) |
| $A_g$ | 277 | 0 | | |
| $B_{2u}$ | 261 | 0 | parity forbidden | |
| $B_{1u}$ | 244 | 2.6 | *z* | <200 |
| | | Triplet–Triplet ($T_1 - T_x$) Transitions | | |
| $B_{1u}(T_1)$ | | | | |
| $B_{3g}$ | 8457 | 0 | *y* | |
| $B_{2u}$ | 908 | 0 | | |
| $B_{3g}$ | 561 | 0.49 | *y* | 670 |
| ...[a] | ... | 0 | | |
| $A_g$ | 243 | 0.9 | *z* | |

[a] No allowed transitions calculated between 561 and 243 nm.

**Table II.** Calculated (CNDO/S) Absorption Spectrum of 1,8-Naphthoquinodimethane ($C_{2v}$ Point Group) in the Lowest Singlet State

| sym | λ/nm | osc strength (*f*) | sym | λ/nm | osc strength (*f*) |
|---|---|---|---|---|---|
| $A_1$ | grnd st | | $A_1$ | 363 | 0.0752 |
| $B_2$ | 1030 | 0.0026 | $B_2$ | 311 | 0.0026 |
| $A_1$ | 504 | 0.0505 | $A_1$ | 297 | 0.0064 |
| $A_1$ | 444 | 0.0026 | $B_2$ | 272 | 0.1302 |
| $B_2$ | 415 | 0.0043 | | | |

method,[6] ignoring the saturated dimethylmethylene bridges (Table I). All 49 singly excited configurations and the lowest doubly excited configuration were included for configuration interaction, and standard parameters used were as follows: resonance integrals $\beta$ = –2.318 eV, repulsion integrals $\gamma_{\mu\nu}$ = 1439.5/(132.8 + $r_{\mu\nu}$/pm) eV, bond lengths 140 pm, bond angles 120°.

Open-shell PPP SCF CI calculations for the triplet–triplet transitions of 1,8-naphthoquinodimethane and naphthalene ($\pi$-systems of **b** and **2**) have previously been reported.[7] The experimental absorption spectra of parent 1,8-naphthoquinodimethane[5k] and of several alkyl derivatives[5a-j] agree very well with the transition energies and intensities calculated by this method. We used the same model to calculate the triplet–triplet transitions of **1** (Table I). B. Dick kindly provided the results of a CNDO/S calculation[8] with extensive CI for both the singlet and the triplet manifold of 1,8-naphthoquinodimethane (Table II; standard CNDO/S parameters, except for $\beta_C$ = –16.0 eV). The energy-selected basis of singly and doubly excited configurations included 200 configurations for the singlet and 300 configurations for the triplet. The reliability of such a calculation for a singlet biradical is questionable; the SCF calculation is performed on a configuration that contributes only 56% to the lowest singlet state, and, more important, the equilibrium geometry may be substantially different from the assumed structure. CNDO/S predictions for the triplet–triplet absorption spectrum are practically identical with those obtained[7] by the PPP method using only 50 configurations.

**Irradiation of 1 and 2 at Room Temperature.** Diffuse daylight or near-UV irradiation rapidly bleaches the yellow solutions of **1**. UV spectroscopic monitoring of the reaction progress in hexane solution indicated a clean and complete reaction with isosbestic points at 248, 285, and 336 nm.[4] Thin layer chromatography of the photoproducts on alumina with cyclohexane separated two compounds, $R_f$ = 0.67 and 0.75, with identical UV and mass spectra. $^1$H-NMR spectroscopy establishes the constitution of both products as 2,2,7,7-tetramethyldicycloprop[*a*,*g*]pyracene (**2**); the spectra of the two geometric isomers *syn*-**2** and *anti*-**2** were nearly identical and consisted of four singlet peaks ($\delta$ = 7.2, 4H; 2.8, 4H; 1.3, 6H; 0.4 ppm, 6H in $CDCl_3$). The slight (≤0.05 ppm) chemical shift differences[4] between the two isomers were sufficient for analysis of their relative yield in the photoproduct mixture; in $CDCl_3$, the two isomers form in a ratio of 1:1 (±3%). We assume that the stereoisomer with the longer retention time ($R_f$ = 0.67) is *syn*-**2** because it has a dipole moment (*vide infra*) and can expose one side of the $\pi$-system to the polar alumina surface without steric hindrance by dimethylcyclopropane moieties.

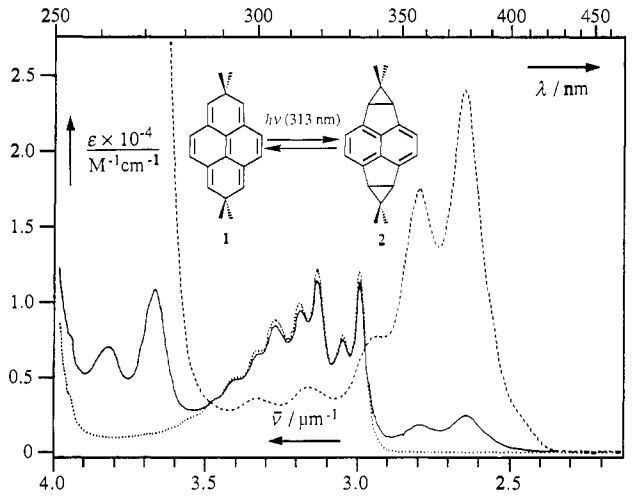


**Figure 1.** Absorption spectra of **1** (- - -), **2** (···), and of the photostationary mixture (—) obtained by 313-nm irradiation of either **1** or **2** in degassed hexane at room temperature.

The quantum yield of the photoreaction **1** → **2** was determined for irradiation at 365 nm, where **2** does not absorb, with degassed, 3.5 × $10^{-5}$ M dichloromethane solutions at room temperature. The progress of the reaction was monitored spectrophotometrically at $\lambda_{max}$(**1**) = 379 nm. Three independent determinations of the extinction coefficient of **1** in dichloromethane gave $\epsilon_{379}$ = (24 100 ± 200) $M^{-1}$ $cm^{-1}$. Actinometry with a 2.5 × $10^{-3}$ M solution of Aberchrome 540 in toluene[9a] gave a quantum yield of 1.1 ± 0.1. Using the same actinometer, we have previously obtained[5g] another quantum yield somewhat exceeding unity; this suggests that the reported quantum yield of Aberchrome 540, $\phi$(365 nm) = 0.20,[9a] is too high by about 10%.[9b] We assume that $\phi_{1\rightarrow2}$(365 nm) is close to unity and not less than 0.9.

Photoinduced valence isomerization is reversible: 313-nm irradiation of either **2** or **1** in hexane yields the same photostationary mixture containing 87% of **2** and 13% of **1** (Figure 1). $^1$H-NMR analysis showed that the two geometric isomers of **2** were present in nearly equal amounts in the photostationary mixtures. Hence, the two geometric isomers *syn*-**2** and *anti*-**2** are equally photoreactive, and quantum yields for the forward and backward reaction relate by eq 1,[10]

$$\phi_{2\rightarrow1} = \frac{\epsilon(\mathbf{1})[\mathbf{1}]_\infty}{\epsilon(\mathbf{2})[\mathbf{2}]_\infty}\phi_{1\rightarrow2} \qquad (1)$$

where $[\mathbf{1}]_\infty$ and $[\mathbf{2}]_\infty$ are the concentrations of **1** and **2** in the photostationary mixture and $\epsilon$(**1**) = 4120 and $\epsilon$(**2**) = 10 960 $M^{-1}$ $cm^{-1}$ are the extinction coefficients at 313 nm of **1** and **2** in hexane. Equation 1 yields $\phi_{2\rightarrow1}$(313 nm) = 0.05 ± 0.01 for the quantum yield for the photoreaction **2** → **1**.

(6) Pariser, R.; Parr, R. G. *J. Chem. Phys.* **1953**, *21*, 466. Pople, J. A. *Trans. Faraday Soc.* **1953**, *49*, 1375.
(7) Gisin, M.; Wirz, J. *Helv. Chim. Acta* **1983**, *66*, 1556.
(8) Dick, B.; Nickel, B. *Chem. Phys.* **1983**, *78*, 1.
(9) (a) Heller, H. G.; Langan, J. R. *J. Chem. Soc., Perkin Trans. 2* **1981**, 341. (b) Very recently we learned that, contrary to the claims in ref 9a, solutions of Aberchrome 540 rapidly age under near-UV irradiation and that this leads to low estimates of light intensities when solutions are used repeatedly. See: Boule, P.; Pilichowski, J. F. *EPA Newsl.* **1993**, *47*, 42. The aging is attributed to *E*/*Z*-isomerization: Yokoyama, Y.; Iwai, T.; Kera, N.; Hitomi, I.; Kurita, Y. *Bull. Chem. Soc. Jpn.* **1990**, 1607.
(10) Wyman, G. M. *Mol. Photochem.* **1974**, *6*, 81.

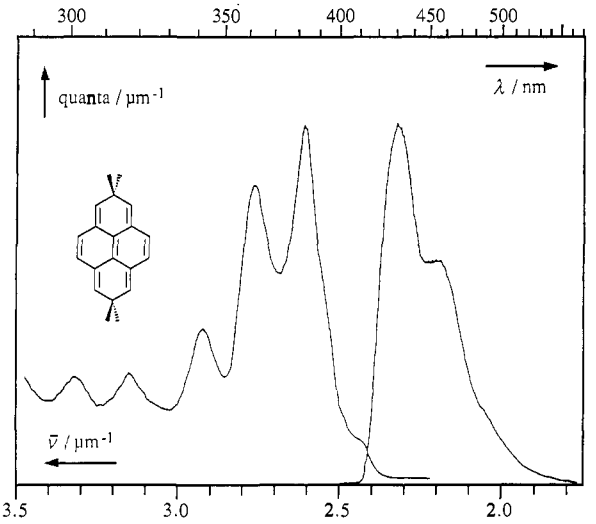


**Figure 2.** Fluorescence excitation and emission spectra of **1** in EPA glass at 77 K.

**Absorption and Emission Spectra of 1 and 2.** The absorption spectrum of **1** (Figure 1) exhibits two strong bands with dominant 1400-$cm^{-1}$ progressions in the near-UV region, $\lambda_{max}$/nm ($\log[\epsilon/M^{-1}\,cm^{-1}]$): 379 (4.38) and 271 (4.91). In addition, two weak maxima appear on the blue tail (300, 315 nm) and a shoulder appears on the red tail (415 nm) on the first absorption band. These features do not fit the main progression of this band and presumably arise from different electronic transitions. Such transitions are predicted by a PPP SCF CI calculation of **1** (Table I). Note that the symmetry-forbidden transition to the lowest excited singlet state of **1** is described by singly excited configurations and bears no relation to the low-lying $A_g$ state found in linear polyenes. The lowest $A_g$ state of **1** is calculated to lie at much higher energies. Attempts to determine band polarizations experimentally by the stretched sheet method[11] failed; the out-of-plane methyl substituents are probably responsible for the poor orientation of **1** in stretched polyethylene sheets, even at 77 K.

The fluorescence of both **1** and **2** is extremely weak in solution at room temperature. However, both compounds are strongly fluorescent at 77 K in EPA glass (ether, isopentane, alcohol; 5:5:2 by volume). The fluorescence spectrum of **1** (Figure 2) exhibits a large Stokes shift and does not obey a mirror-image relationship to the absorption spectrum. This supports our assignment of the weak shoulder on the red edge of the first absorption band to a separate electronic transition. The fluorescence excitation spectrum of **1** was superimposable with the absorption spectrum.

The quantum yield of fluorescence of **1** at 77 K was determined by comparing the area of the corrected emission spectrum with that of 9,10-diphenylanthracene (DPA), the fluorescence quantum yield of which is very close to unity at 77 K.[12] DPA was excited at 374.5 nm and **1** at 382.5 nm, using light of 1-nm bandwidth from a xenon arc lamp; the relative intensity of the excitation source at the two wavelengths was monitored with a Rhodamine 6G quantum counter. This gave $\phi_{Fl}(\mathbf{1}) = 0.7 \pm 0.1$ for the fluorescence quantum yield of **1** at 77 K in EPA glass. A similar determination with a hydrocarbon glass (2,2-dimethylbutane, pentane; 8:3 by volume) at 77 K gave identical results, $\phi_{Fl}(\mathbf{1}) = 0.7 \pm 0.1$.

Frequency-tripled, 355-nm pulses from a Nd–glass laser were chopped to about 5-ns half-width with a gated Pockels cell and used to determine the fluorescence lifetime of **1** in EPA at 77 K. First-order analysis of the fluorescence decay curves gave $\tau_{Fl} = 17 \pm 1$ ns. The fluorescence rate constant, calculated as $k_{Fl} = \phi_{Fl}/\tau_{Fl} = (4.1 \pm 0.6) \times 10^7\ s^{-1}$, is a factor of 3 lower than that predicted by integration of the entire absorption band ($\lambda_{max}$ = 382.5 nm in EPA), using the Strickler–Berg approximation.[13] This again supports our *assignment of the fluorescent $S_1$ state of **1** to a $B_{3g}$ state* (Table I).

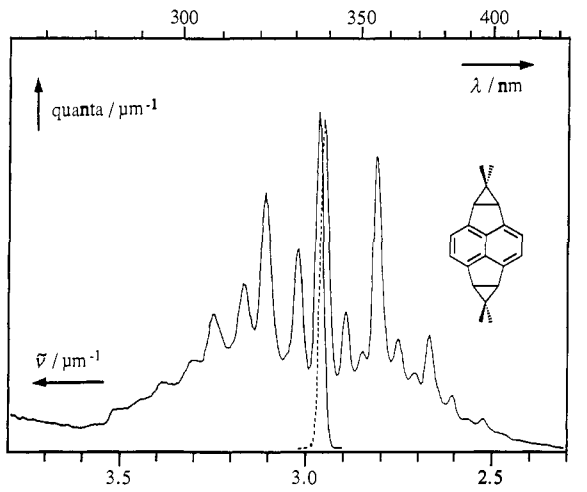


**Figure 3.** Fluorescence excitation and emission spectra of **2** in EPA glass at 77 K.

Excitation of **1** in a hydrocarbon, glassy matrix at 77 K further gave rise to a very weak phosphorescence emission with a lifetime $\tau_{Ph} = 19 \pm 1$ ms. The 0–0 band of this emission was at 803 nm, corresponding to a triplet energy of 149 kJ $mol^{-1}$.

The fluorescence of **1** at room temperature was too weak for detection on a standard fluorescence spectrometer. It was, however, readily observed upon pulsed-laser excitation (XeCl excimer laser, 308 nm, ca. 150 mJ per pulse) using a diode array detector with a gated image intensifier. The fluorescence quantum yield of **1** in hexane solution at ambient temperature was estimated using a highly dilute solution of DPA in hexane as a standard ($\phi_{Fl}$ = 0.9).[12] The fluorescence spectra of **1** and DPA were nearly superimposable, obviating the need to correct for spectral sensitivity of the detection system. This gave $\phi_{Fl}(\mathbf{1}) = (9 \pm 3) \times 10^{-5}$, consistent with the near unit quantum efficiency of photoisomerization. Assuming that the radiative rate constant determined at 77 K holds for room temperature, *we estimate the lifetime of the lowest singlet state of **1** as $\tau_{Fl}(\mathbf{1}, 298\ K) = \phi_{Fl}(\mathbf{1})/k_{Fl} = 2.4 \pm 1.0$ ps.*

To assign the electronically excited singlet states of the two isomers of **2**, we consider these molecules as substituted naphthalenes. Fusion of one dimethylcyclopropane group to the *peri* position of naphthalene gives 7,7-dimethyl-6b,7a-dihydro-7*H*-cycloprop[*a*]acenaphthylene (**4**).[5g] The $^1L_a$ band of **4** is red-

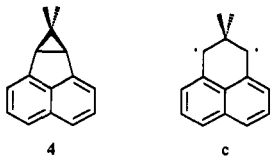

4 c

shifted by ca. 3600 $cm^{-1}$ relative to that of naphthalene, whereas the position of the $^1L_b$ band is hardly affected (ca. 200-$cm^{-1}$ red shift); the $^1L_b$ state of **4** is still the lowest excited singlet state ($S_1$, $\tilde{\nu}_{0-0}$ = 30 800 $cm^{-1}$), but its separation from the $^1L_a$ state ($S_2$) is only 300 $cm^{-1}$.[5g] If these perturbations are simply additive in doubly fused compounds **2**, we expect the $^1L_a$ state to be the lowest excited singlet state ($S_1$, $\tilde{\nu}_{0-0} \cong 27\,500\ cm^{-1}$), the $^1L_b$ state now being the $S_2$ state. The 0–0 transition of the $S_0$–$S_1$ ($^1L_a$) band of **2** is at somewhat higher frequency than predicted by this simple estimate, $\tilde{\nu}_{0-0} \cong 29\,500\ cm^{-1}$ (Figure 3). Under the $C_{2v}$ point group for *syn*-**2**, the state symmetry assignments are

(11) Michl, J.; Thulstrup, E. W. *Spectroscopy with Polarized Light*; VCH Publishers, Inc.: New York, 1986. Phillips, P. J. *Chem. Rev.* **1990**, *90*, 425.
(12) Morris, J. V.; Mahaney, M. A.; Huber, J. R. *J. Phys. Chem.* **1976**, *80*, 969. Mantulin, W. W.; Huber, J. R. *Photochem. Photobiol.* **1973**, *17*, 139.
(13) Strickler, S. J.; Berg, R. A. *J. Chem. Phys.* **1962**, *37*, 814.

$S_1(^1L_a)$:$B_2$, $S_2(^1L_b)$:$B_1$. Under $C_{2h}$ for *anti*-**2**, they are $S_1(^1L_a)$: $B_u$, $S_2(^1L_b)$:Au. With respect to the common plane of symmetry ($C_s$ point group), the $S_1$ state ($^1L_a$) is symmetric; the $S_2$ state ($^1L_b$) is antisymmetric.

The fluorescence of **2** is very weak at room temperature, $\phi_{Fl} \lesssim 10^{-4}$, but quite strong at low temperature. The fluorescence spectrum of **2** (1:1 mixture) in EPA at 77 K roughly obeys a mirror-image relationship to the first absorption band (Figure 3), but the vibrational fine structure is more pronounced in the emission. This may arise from overlap of the $^1L_a$ absorption band with the $^1L_b$ band (onset expected at ca. 30 600 $cm^{-1}$). We could not detect any phosphorescence of **2**. The strong temperature dependence of the fluorescence yield of **2** indicates that a thermally activated chemical process competes with fluorescence. This process is attributed to ring cleavage forming the singlet biradical $^1$**b**, similar to the fission of naphthocyclopropane **4** yielding $^1$**c**.[5g] Positive evidence for this hypothesis will be given below (picosecond flash photolysis).

**Photoelectron Spectrum of 1.** A sample of **1** was sublimed at ca. 125 °C near the ionization chamber. The He I photoelectron spectrum exhibited two well-separated, sharp peaks, $I_{v,1}$ = 6.70 and $I_{v,2}$ = 7.50 eV, followed by two broad peaks, $I_{v,3} \cong 9.0$ eV and $I_{v,4} \cong 9.8$ eV. The latter was at the onset of the congested region of overlapping $\sigma$-ionizations. The $\pi$-orbital energies of **1** obtained by the PPP SCF calculation described above,[14] $\epsilon_1(b_{3u})$ = −6.65, $\epsilon_2(b_{1g})$ = −7.49, $\epsilon_3(b_{3u})$ = −9.17, and $\epsilon_4(a_u)$ = −9.78 eV, are in excellent agreement with the observed ionization energies, $I_{v,n} \cong -\epsilon_n$ (Koopmans' theorem; axis convention for orbital symmetry assignments under $D_{2h}$:*y* and *z* in the plane of the $\pi$-system, *z* parallel to double bonds). We could not measure the photoelectron spectrum of **2** because isomerization to **1** occurred on heating before a sufficient vapor pressure was reached.

**Irradiation at 77 K, Optical and ESR Spectra of $^3$b.** In sharp contrast to the results at room temperature, **1** was stable to prolonged photolysis in EPA glass at 77 K, $\phi_{1\to2}$(77 K) < 0.001, and the photostationary equilibrium reached by irradiation of **2** at 313 nm was entirely on the side of **1**. The UV spectral changes occurring during the slow photochemical transformation of **2** to **1** were analyzed by the spectrophotometric method of Mauser,[15] which revealed that conversion took place in two sequential photoreactions (curved *ED* diagrams, linear *EDQ* diagrams). The photochemical reactivity of the primary photoproduct was much higher than that of **2**, such that its concentration remained low throughout the photolysis. Nevertheless, pronounced curvature appeared in the *ED* diagrams[15] at monitoring wavelengths in the range of 330–350 nm, indicating that the intermediate absorbs predominantly in that region. Very weak, highly structured absorption of the intermediate around 500 nm was also noticeable.

The intermediate also exhibited green fluorescence emission that allowed us to determine its absorption spectrum in the reaction mixture as an excitation spectrum of the green emission (Figure 4). This spectrum is very similar to that of related 1,8-naphthoquinodimethane triplet biradicals[5] and is attributed to triplet biradical $^3$**b**. When we irradiated a sample of **2** under liquid $N_2$ and transferred it to the cooled cavity of an ESR spectrometer, we detected the signal shown in Figure 5, which proves that a triplet with zero-field parameters $|D/hc|$ = 0.028 ± 0.002 $cm^{-1}$ and $|E/hc| \lesssim 0.001$ $cm^{-1}$ had been formed. These values are similar to those of related perinaphthadiyl biradicals.[5] The variation of the ESR signal intensity obeyed Curie's law (*I* × *T* ≈ const) in the temperature range from 2.8 to 15 K, indicating that *the triplet state is the electronic ground state of* **b**.[16]

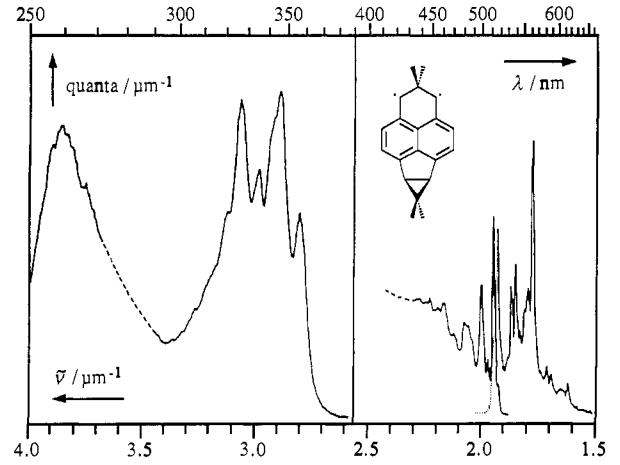


**Figure 4.** Fluorescence excitation and emission spectra of $^3$**b** generated by 313-nm irradiation of **2** in EPA glass at 77 K. The weak excitation spectrum in the visible region was determined in a separate experiment using a higher concentration. Approximate extinction coefficients for the UV and vis bands were obtained from the analysis of absorbance changes during irradiation (see text): $\log(\epsilon/M^{-1}\,cm^{-1}) \approx 4.6$ at 325 and 345 nm and ≈3.2 at 510 nm.

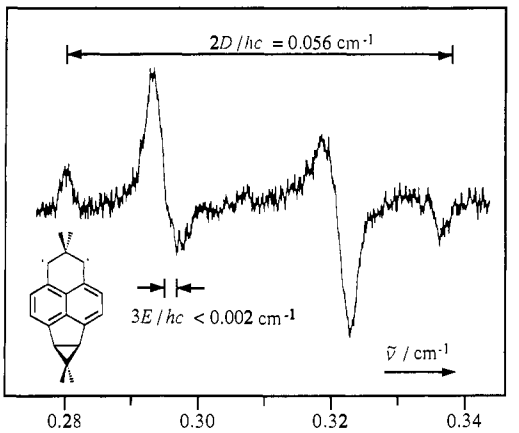


**Figure 5.** ESR spectrum of $^3$**b** generated by 313-nm irradiation of **2** in EPA glass at 77 K.

**Thermal Isomerization.** As mentioned above, geometrical isomers *syn*-**2** and *anti*-**2** were formed in equal yield when a solution of **1** in $CDCl_3$ was irradiated at room temperature. Chromatography readily separates the two isomers of **2**, but they slowly reequilibrate in solution at room temperature. $^1$H NMR was used to determine the kinetics of the ring-flip reaction *anti*-**2** → *syn*-**2**. Four samples of pure *anti*-**2** (2 mg in 0.4 mL of $CDCl_3$ each) were kept in a thermostat (25, 30, 35, 40 ± 0.1 °C) and their NMR spectra recorded at regular intervals. Spectra were taken at 0 °C to avoid reaction during the periods of analysis; five or six spectra were taken of each sample. The kinetics obeyed a first-order rate law, as expected for the reversible equilibration *anti*-**2** ⇄ *syn*-**2**, eq 2,

$$\ln\left(\frac{[anti\text{-}2]_0 - [anti\text{-}2]_\infty}{[anti\text{-}2]_t - [anti\text{-}2]_\infty}\right) = k_{obs} \times t = (k_{a\to s} + k_{s\to a}) \times t \quad (2)$$

and the observed rate constants, $k_{obs} = k_{a\to s} + k_{s\to a}$, were (5.4

(14) The value $I_C$ = 9.8 eV for the valence-state ionization potential of carbon was taken from Clark, P. A.; Brogli, F.; Heilbronner, E. *Helv. Chim. Acta* **1972**, *55*, 1415.

(15) Mauser, H. Z. *Naturforsch.* **1968**, *23b*, 1025.

(16) Analysis of the data by nonlinear least-squares fitting to the Boltzmann distribution appropriate for a triplet in thermal equilibrium with a singlet ground state gave an energy gap, $\Delta E_{ST}$ = 0.026 kJ $mol^{-1}$. As in previous cases,[5g] we attribute this very minor nonlinearity to systematic errors arising from saturation effects and/or errors in the temperature readings, and we consider the results as being consistent with Curie's law within experimental accuracy.

(17) Braslavsky, S. E.; Heibel, G. E. *Chem. Rev.* **1992**, *92*, 1381.

**Table III.** Solvent Dependence of the Thermal Equilibrium *anti*-**2** ⇄ *syn*-**2**

| solvent | $T$/K | $K = [syn\text{-}2]/[anti\text{-}2]$ | $(\epsilon - 1)/(2\epsilon + 1)$ |
|---|---|---|---|
| cyclohexane-$d_{12}$ | 298 | 0.93 ± 0.02 | 0.20 |
| cyclohexane-$d_{12}$ | 348 | 1.01 ± 0.02 | |
| $CDCl_3$ | 298 | 1.13 ± 0.02 | 0.36 |
| $CDCl_3$ | 313 | 1.15 ± 0.02 | |
| acetone-$d_6$ | 298 | 1.27 ± 0.02 | 0.46 |
| DMSO-$d_6$ | 298 | 1.65 ± 0.10 | 0.48 |

**Table IV.** Summary of Experimentally Determined Rate Constants (25 °C)

| reaction | solvent | rate const |
|---|---|---|
| $S_1(1) \rightarrow {}^1\mathbf{b}$ | hexane | $(3.3 \pm 0.3) \times 10^{11}$ s$^{-1}$ |
| $T_1(1) \rightarrow \mathbf{1}$ | $C_6H_6$, EtOH; 2:1 | $(3.2 \pm 0.2) \times 10^{3}$ s$^{-1}$ |
| *anti*-**2** → *syn*-**2** | $CDCl_3$ | $(2.8 \pm 0.2) \times 10^{-5}$ s$^{-1}$ [a] |
| *syn*-**2** → *anti*-**2** | $CDCl_3$ | $(2.6 \pm 0.2) \times 10^{-5}$ s$^{-1}$ [b] |
| **2** → **1** | dodecane | $(6 \pm 1) \times 10^{-9}$ s$^{-1}$ [c] |
| **2** + $^3O_2$ → **3** + ... | hexane | $(1.8 \pm 0.6) \times 10^{-4}$ M$^{-1}$ s$^{-1}$ |
| $^3$**b** → **2** | $CH_3CN$ | $(1.5 \pm 0.1) \times 10^{3}$ s$^{-1}$ [d] |
| $^3$**b** + $^3O_2$ → **3** + ... | $C_6H_6$ | $(1.3 \pm 0.1) \times 10^{9}$ M$^{-1}$ s$^{-1}$ |
| $^1$**b** → **2** | hexane | $(5.6 \pm 0.3) \times 10^{10}$ s$^{-1}$ |

[a] Activation parameters log ($A$/s$^{-1}$), $E_a$/(kJ mol$^{-1}$), temperature range: 13.3 ± 0.5, 102 ± 5, 25–40 °C. [b] 13.1 ± 0.5, 101 ± 5, 25–40 °C. [c] 12.6 ± 0.5, 119 ± 5, 95–110 °C. [d] 7.7 ± 0.5, 26 ± 2, 95–110 °C.

± 0.2) × 10$^{-5}$ (25.0 °C), (1.10 ± 0.02) × 10$^{-4}$ (30.0 °C), 2.15 ± 0.05) × 10$^{-4}$ (35.0 °C), and (3.8 ± 0.1) × 10$^{-4}$ s$^{-1}$ (40.0 °C). The ratio of *syn*-**2** to *anti*-**2** after prolonged equilibration in $CDCl_3$ at 25 °C was 1.13 ± 0.02, which is slightly, but significantly, different from that of the 1:1 mixture obtained by irradiation of **1**. The temperature dependence of $K = [syn\text{-}2]/[anti\text{-}2]$ is quite small (Table III). Arrhenius parameters determined from $k_{obs}(T)$ and $K(T)$ are given in Table IV.

On the other hand, we found that the equilibrium depends markedly on solvent polarity; the equilibrium constant $K$(298 K) shifts from 0.93 in cyclohexane-$d_{12}$ to 1.65 in dimethyl sulfoxide-$d_6$ (Table III). This supports our assignment of the geometric isomers of **2**, since the dipole moment of *anti*-**2** must vanish under $C_{2h}$ symmetry. The available quantities of **2** were too small to determine the dipole moments of the isomers directly, but a crude estimate of the difference $\Delta\mu$ can be obtained from the solvent dependence of the equilibrium through the so-called Kirkwood relation (3)

$$\Delta G^{\ominus} = -RT \ln K = -\left(\frac{N_A}{4\pi\epsilon_0}\right)\left(\frac{\Delta\mu^2}{a^3}\right)\left(\frac{\epsilon - 1}{2\epsilon + 1}\right) \quad (3)$$

where $\epsilon$ is the dielectric constant of the solvent and $a$ is the "radius" of solute **2**. With $a \approx 500$ pm, we obtain $\Delta\mu \approx 2.5$ D from the data given in Table III.

Quantitative valence isomerization of **2** to **1** occurred in the dark at elevated temperatures. Four samples of **2** in degassed dodecane were kept in a thermostat (95, 100, 105, 110 ± 0.15 °C) and their UV spectra recorded at regular intervals. At these temperatures, the equilibrium *anti*-**2** ⇄ *syn*-**2** is established rapidly. The observed first-order rate constant for isomerization then corresponds to the combination of rate constants shown in the right-hand term of eq 4

$$\ln\left(1 - \frac{[\mathbf{1}]_t}{[\mathbf{1}]_\infty}\right) = k_{obs} \times t = -\left(\frac{Kk_{a\rightarrow 1} + k_{s\rightarrow 1}}{K + 1}\right) \times t \quad (4)$$

where $K = k_{a\rightarrow s}/k_{s\rightarrow a}$ is the equilibrium constant for the geometric isomerization *anti*-**2** ⇄ *syn*-**2** and $k_{a\rightarrow 1}$ and $k_{s\rightarrow 1}$ are the individual rate constants for the conversion of *anti*- and *syn*-**2**, respectively, to **1**. Analysis of these data gave $k_{obs} = (5.70 \pm 0.06) \times 10^{-5}$ (95 °C), (9.84 ± 0.09) × 10$^{-5}$ (100 °C), (1.56 ± 0.02) × 10$^{-4}$ (105 °C), and (2.62 ± 0.01) × 10$^{-4}$ s$^{-1}$ (110 °C) from which Arrhenius parameters log ($A$/s$^{-1}$) = 12.6 ± 0.5 and $E_a$ = 119 ± 5 kJ mol$^{-1}$ were obtained by linear regression. Extrapolation to 25 °C gives $k_{obs} \cong 6 \times 10^{-9}$ s$^{-1}$, i.e., *the isomerization* **2** → **1** *is 4 orders of magnitude slower at room temperature than the ring-flip reaction anti-***2** ⇄ *syn-***2**.

**Thermochemical Data.** The heat of reaction **2** → **1** was determined by differential scanning calorimetry (DSC). Preliminary experiments with solid **2** showed that melting and isomerization of **2** took place simultaneously around 150 °C (depending on the rate of heating). On the other hand, the solubility of **2** in various solvents at ambient temperature was insufficient for reliable DSC measurements. A sufficient amount of **2** (0.5 mg) could be dissolved in 1,2,4-trichlorobenzene (10 μL) by preheating the mixture for 2 h at 80 °C. Subsequent heating to 170 °C at a rate of 5 °C s$^{-1}$ gave a strong exothermic signal due to the reaction **2** → **1**. Small corrections were applied to account for the amount of material isomerized during the preheating period (11 ± 2%), for incomplete isomerization (product analyses of the pyrolyzed samples indicated ≥90% conversion), and for a small amount of irreversible decomposition of **1** (the signal drift observed by heating **1** under identical conditions was used as a base line). Four independent runs gave an average heat of reaction $\Delta_{2\rightarrow 1}H_m(425\text{ K}) = -61 \pm 4$ kJ mol$^{-1}$ (ca. 2 M in 1,2,4-trichlorobenzene). Contributions from systematic errors should be within ±10 kJ mol$^{-1}$.

Photoacoustic calorimetry (PAC)[17] provided a completely independent measurement of the same heat of reaction (at 20 °C). Photoacoustic signals obtained by pulsed-laser excitation (351 nm) of **1** (3 × 10$^{-4}$ M) in aerated acetonitrile had the same shape as but were less intense than the reference signals of 2-hydroxybenzophenone in the same solvent. This indicates that the photoisomerization **1** → **2** is much faster than the 25-ns duration of the laser pulse and that it is an energy-storing process. Analysis of the traces for a single, fast process of heat evolution (1 ns was arbitrarily assumed for both reference and sample) gave a good fit to the transducer response in the time range of 0–2 μs and showed that only (76 ± 3)% of the absorbed light energy appeared as heat in the sample. Fitting with more than one exponential did not improve the goodness of fit. With the value of unity determined above for the quantum yield of photoisomerization $\phi_{1\rightarrow 2}$, this corresponds to a heat of 82 ± 15 kJ mol$^{-1}$ stored in the process **1** → **2**. Giving equal weight to PAC and DSC values, we obtain a mean *value of 72 ± 10 kJ mol$^{-1}$ as our best estimate for the enthalpy change associated with the reaction* **1** → **2** *in solution.*

**Nanosecond Flash Photolysis, Detection of Triplet Intermediates in Solution.** Direct excitation of either **1** or **2** at ambient temperature with a 20-ns laser pulse gave no transient absorption. As described below, long-lived triplets *were* observed by triplet sensitization of these compounds. Hence, spontaneous ISC to the triplet manifold must be inefficient, i.e., *the photoisomerization* **1** ⇄ **2** *is predominantly a singlet-state reaction at ambient temperature.*

We chose Rose Bengal B (Fluka) as a triplet sensitizer for **1** because it allows for selective excitation of the sensitizer in the visible region, its triplet–triplet absorption spectrum is known,[18] and its triplet energy (164 kJ mol$^{-1}$)[19] is higher than that of **1** determined from phosphorescence emission ($E_T$ = 149 kJ mol$^{-1}$). Flash photolysis with the frequency-doubled pulse of a Nd–glass laser (532 nm, 20-ns pulse width) showed that the triplet state of Rose Bengal was quenched at a near diffusion-controlled rate by **1** in a degassed 2:1 mixture of benzene and ethanol and that a new, long-lived transient absorption appeared at the same rate around 650 to 700 nm ($\lambda_{max}$ = 670 nm, no other absorption in the visible region). This transient is attributed to the lowest triplet state of **1**; its lifetime, $\tau$ = 310 ± 20 μs, was determined using a conventional discharge flash for excitation ($\lambda > 450$ nm) at low power to avoid second-order contributions to the decay from triplet–triplet annihilation.

(18) Grajcar, L.; Ivanoff, N.; Delouis, J. F.; Faure, J. *J. Chim. Phys. France* **1984**, *81*, 33.
(19) Gollnik, K. In *Adv. Photochem.*; Noyes, W. A., Jr., Hammond, G. S., Pitts, J. N., Jr., Eds.; Interscience Publishers: New York, 1968; Vol. 6, Chapter 1, p 14.

Sensitization of **1** was also possible through anthracene as a triplet energy relay: when the triplet of Rose Bengal was quenched by excess anthracene ($3 \times 10^{-3}$ M), subsequent energy transfer to **1** could be observed by quenching of the anthracene triplet ($\lambda_{max}$ = 424 nm)[20] and concomitant growth of the 670-nm triplet absorption of **1**. The rate of energy transfer from triplet anthracene to **1**, $k_{et} = (1.0 \pm 0.5) \times 10^9$ $M^{-1}$ $s^{-1}$, was somewhat short of diffusion control, suggesting that the triplet energy of **1** is not much below that of anthracene ($E_T$ = 178 kJ $mol^{-1}$).[21] With dibenzo[*a*,*h*]pyrene (DBP, K&K rare chemicals) as a triplet sensitizer ($E_T$ = 144 kJ $mol^{-1}$),[22] energy transfer from $^3$DBP to **1** was reversible, establishing an equilibrium before the decay of both triplets. In a degassed solution of benzene containing $3.2 \times 10^{-4}$ M **1** and $2.1 \times 10^{-5}$ M DBP, the equilibrium was established within 50 $\mu$s after flash photolysis ($\lambda_{exc}$ > 450 nm); thereafter, the decay rates of $^3$DBP (520 nm) and of $^3$**1** (670 nm) were equal. The extinction coefficient of $^3$DBP in benzene solution at $\lambda_{max}$ = 520 nm[23] was determined as $\epsilon_{520}$ = 23 000 ± 5000 $M^{-1}$ $cm^{-1}$ by energy transfer from triplet anthracene as a standard ($\epsilon_{430}$ = 45 500 $M^{-1}$ $cm^{-1}$).[24] The absorbance of $^3$DBP diminished from $A$ = 0.25 to $A$ = 0.06 during the initial equilibration. The absorbance of $^3$**1** reached a maximum of $A$ = 0.06 after equilibration. Hence, the extinction coefficient of $^3$**1** at 670 nm is about one-third that of $^3$DBA at 520 nm, i.e., $\epsilon_{670}(^3\text{DBA})$ = 8000 ± 3000 $M^{-1}$ $cm^{-1}$. From these data, the equilibrium constant $K$ = [DBP][$^3$**1**]/{[**1**][$^3$DBP]} is calculated to lie within the range of 0.1–0.4, i.e., the free energy change associated with triplet energy transfer from $^3$DBP to **1** is slightly positive, $\Delta_{et}G^{\ominus} = 4 \pm 2$ kJ $mol^{-1}$. *These experiments bracket the triplet energy in the range of $E_T$(**1**) = 148 ± 2 kJ $mol^{-1}$*, in excellent agreement with the energy of 149 kJ $mol^{-1}$ determined by phosphorescence emission. As expected, energy transfer from $^3$**1** to tetracene ($E_T$ = 123 kJ $mol^{-1}$)[21] was irreversible and nearly diffusion-controlled, $k_{et} = (3.4 \pm 1) \times 10^9$ $M^{-1}$ $s^{-1}$. Triplet sensitization of **1** did not result in any chemical change such as isomerization to **2** or oxidation in aerated solution.

Triplet sensitization of **2** was first done with benzophenone ($E_T$ = 285 kJ $mol^{-1}$).[21] Quenching of triplet benzophenone by **2** was close to diffusion-controlled in degassed acetonitrile solution, $k_{et} = 5 \times 10^9$ $M^{-1}$ $s^{-1}$, and a new transient intermediate appeared with strong absorbance in the range of 320–360 nm and a lifetime exceeding 100 $\mu$s. This transient was clearly not due to the triplet state of **2** that ought to show triplet–triplet absorption similar to naphthalene.[20] Rather, the spectrum was characteristic of triplet biradical intermediate $^3$**b** (Figure 4). At sufficiently high concentrations of **2**, the transient absorption of $^3$**b** appeared within 100 ns, indicating a short lifetime of the triplet state formed initially by energy transfer from triplet benzophenone to **2**.

State-symmetry analysis predicts that the formation of $^3$**b** occurs from an upper triplet state of **2** (cf. Discussion). To test this prediction, we used chrysene as a low-energy sensitizer ($E_T$ = 238 kJ $mol^{-1}$).[21] The triplet–triplet absorption of chrysene ($\lambda_{max}$ = 570 nm),[20] observed after 351-nm laser flash photolysis of chrysene, was quenched in the presence of $2.1 \times 10^{-3}$ M **2**, $k_{et} = 3.0 \times 10^9$ $M^{-1}$ $s^{-1}$, and a new, long-lived ($\tau$ > 10 $\mu$s) transient absorption, Figure 6, similar in structure to the triplet–triplet absorption of naphthalene[20] but shifted to longer wavelengths grew in at the same rate. The observation of further energy transfer to tetracene (ca. $1 \times 10^{-5}$ M, triplet–triplet absorption $\lambda_{max}$ = 460 nm)[20] identified this transient as a triplet with an excitation energy exceeding 120 kJ $mol^{-1}$. We attribute this transient to the lowest triplet state $T_1$(**2**) and conclude that *the adiabatic reaction from an upper triplet state of **2** to $^3$**b** is faster than radiationless conversion to the lowest triplet state after sensitization with the high-energy triplet donor benzophenone.*

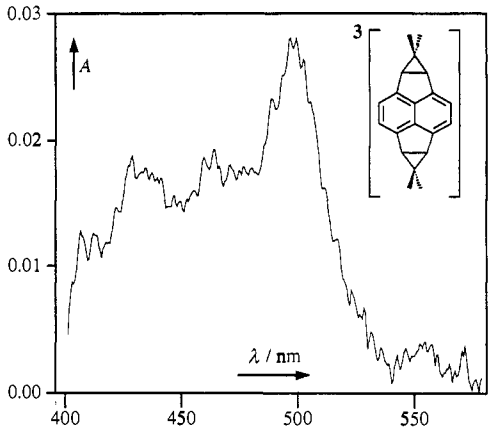


**Figure 6.** Triplet–triplet absorption spectrum of $T_1$(**2**) generated by 351-nm flash photolysis of chrysene in the presence of $2.1 \times 10^{-3}$ M **2** in degassed benzene solution. The transient spectrum was recorded with a delay of 2 $\mu$s relative to the laser flash to allow for complete energy transfer from triplet chrysene to **2**.

The decay rate of $^3$**b** was determined by excitation of the sensitizer with a conventional discharge flash at low power to avoid second-order contributions from triplet–triplet annihilation. Temperature was regulated in the range of 18–56 °C using a water-jacketed sample cell connected to a thermostat. Temperature readings taken directly from the sample solution were within ±1 °C of the specified value. A sufficiently high concentration of **2** ($6 \times 10^{-4}$ M) was used such that energy transfer from triplet benzophenone was virtually complete within the duration of an excitation pulse of 20 $\mu$s. Linear least-squares fitting of 33 data points to the Arrhenius equation gave the following parameters for the decay of $^3$**b**: $\log(A/s^{-1}) = 7.7 \pm 0.2$, $E_a = 25.8 \pm 1.3$ kJ $mol^{-1}$. Such low $A$ factors appear to be typical for the thermal decay of triplet perinaphthadiyl biradicals[5] and indicate that the spin barrier contributes to the unusually long lifetimes of these triplet biradicals. The lifetime of $^3$**b** in degassed acetonitrile at 25 °C was 660 $\mu$s. In benzene saturated with 136 Torr of air, the lifetime of $^3$**b** decreased to 2.2 ± 0.2 $\mu$s. The concentration of oxygen in such a solution is $3.4 \times 10^{-4}$ M;[25] hence, the bimolecular rate constant for oxygen quenching of triplet $^3$**b** is $(1.3 \pm 0.1) \times 10^9$ $M^{-1}$ $s^{-1}$. This quenching of $^3$**b** by oxygen is a chemical-trapping process: sensitization with benzophenone in the absence of oxygen did not consume **2**, but a mixture of oxidation products formed when **2** was sensitized in aerated solution.

**Picosecond Flash Photolysis, Detection of Singlet Biradical $^1$b in Solution.** The transient absorption spectra shown in Figure 7 were observed after excitation of a $3 \times 10^{-4}$ M solution of **2** in hexane with a subpicosecond pulse at 248 nm. The last spectrum ($\Delta t$ = 85 ps) already corresponds to the final difference spectrum arising from the conversion of a small amount of **2** to isomer **1**; it exhibits positive absorption peaks, $\lambda_{max}$ = 378, 358, and ca. 340 nm, indicating the formation of **1**, and weak negative peaks at 334 and 319 nm, indicating the depletion of starting material **2** (compare with Figure 1). The spectra at shorter time delays show stronger absorbance changes in the near-UV that appear to consist of a broad absorption band, $\lambda_{max} \lesssim 345$ nm, overlapping with strong bleaching due to depletion of **2**. Note in particular the sharp onset of bleaching at 340 nm, which coincides with the sharp onset of the first absorption band of **2**. Most of the initially depleted starting material reappears during the first 85 ps after excitation. The broad absorption band $\lambda_{max} \lesssim 345$ nm is attributed

(20) Porter, G.; Windsor, M. W. *Proc. R. Soc. London, A* **1958**, *245*, 238. Carmichael, I.; Hug, G. L. *J. Phys. Chem. Ref. Data* **1986**, *15*, 1.
(21) Birks, J. B. *Photophysics of Aromatic Molecules*; Wiley: London, 1970.
(22) Muel, B.; Hubert-Habart, M. *Adv. Mol. Spectrosc., Proc. Int. Meet., 4th, 1959(1962)* **1962**, *2*, 647. We have redetermined the phosphorescence of DBP and have observed $\lambda_{0-0}$ = 825 nm and $E_T$ = 144 kJ $mol^{-1}$, in excellent agreement with the reported value.
(23) Slifkin, M. A.; Walmsley, R. H. *Photochem. Photobiol.* **1971**, *13*, 57.
(24) Bonneau, R.; Carmichael, I.; Hug, G. L. *Pure Appl. Chem.* **1991**, *63*, 289.
(25) Wilhelm, E.; Battino, R. *Chem. Rev.* **1973**, *73*, 1. Battino, R.; Rettich, T. R.; Tominaga, T. *J. Phys. Chem. Ref. Data* **1983**, *12*, 163.

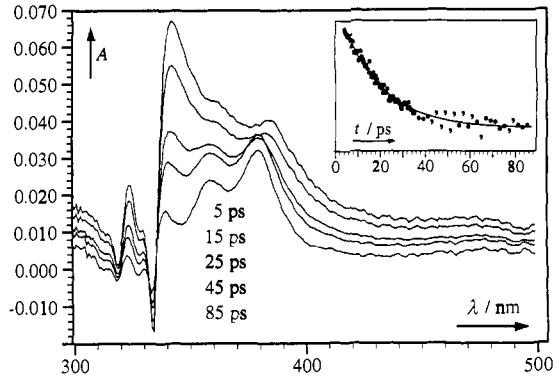


**Figure 7.** Transient absorption spectra observed at several delay times after 248-nm picosecond excitation of **2** in hexane. The inset shows the time evolution of the first eigenspectrum obtained by singular value decomposition of 89 spectra (400 accumulations each) taken at intervals of 0.5 ps up to 37 ps and of 2 ps up to 85 ps. The solid line represents the global kinetic fit to a single exponential.

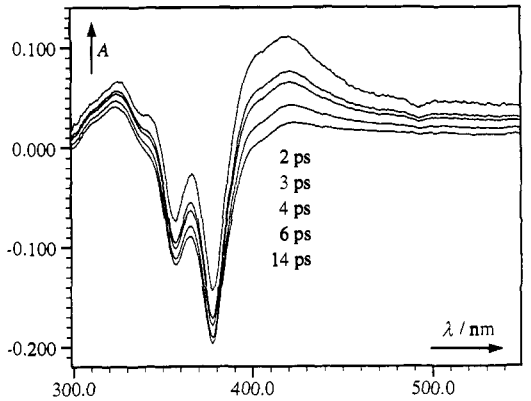


**Figure 8.** Transient absorption spectra observed up to 14 ps after 248-nm excitation of **1** in hexane.

to singlet biradical $^1$**b**. Singular value decomposition of 89 transient spectra taken at intervals of 0.5 ps up to a delay of 37 ps and of 2 ps from 37 to 85 ps gave satisfactory fits to a single exponential with a rate of $(5.6 \pm 0.3) \times 10^{10}$ s$^{-1}$ (inset of Figure 7) corresponding to a lifetime for $^1$**b** of 18 ± 2 ps. Spectral changes in the range of 340–390 nm give some indication of minor contributions by a faster process with a rate of ca. $1 \times 10^{11}$ s$^{-1}$. These initial changes may arise from vibrational relaxation of the hot primary photoproducts. Notably, the peaks around 350 and 380 nm, which are attributed to photoproduct **1**, already appear in the first spectra, though initially they are broadened and slightly red-shifted. Thus, photoproduct **1** forms during the first picoseconds after excitation of **2**, and vibrationally relaxed biradical intermediate $^1$**b** decays predominantly to starting material **2**.

Pulsed excitation of a $2 \times 10^{-4}$ M solution of **1** in hexane induces strong spectral changes during the first 14 ps, as shown in Figure 8. Most obvious is the strong, immediate bleaching of the starting material which is permanent, $\lambda_{max}$ = 378, 358, and ca. 340 nm. It is overlaid by a strong, very broad absorption band ($\lambda_{max} \lesssim 400$ nm, onset ca. 500 nm) which decays with a lifetime of 3.0 ± 0.3 ps. This is close to the fluorescence lifetime of **1**, which was estimated as 2.4 ± 1.0 ps, and the transient is therefore attributed to absorption by the lowest excited singlet state $S_1$(**1**). Further changes of the transient spectra occur after the decay of $S_1$(**1**), as can be seen by comparing spectra recorded with delays of 15 and 55 ps (Figure 9). The half-life of these spectral changes is about 20 ps, accurate analysis being impeded by the overwhelming, if constant, signal arising from the bleaching of **1**. The spectral features and time scale at these transient changes are the same as those found by flash photolysis of **2** and are again attributed to the decay of singlet biradical $^1$**b** yielding **2**.

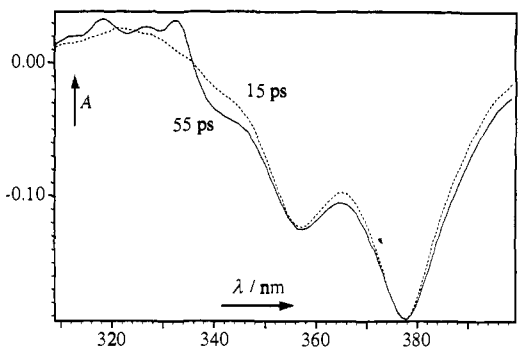


**Figure 9.** Transient absorption spectra observed at 15 ps (dashed line) and 55 ps (solid line) after 248-nm excitation of **1** in hexane.

**Autoxidation of 2.** Solutions of **2** in hexane slowly decomposed in the dark in the presence of oxygen. Oxidation was monitored over a period of 3 mo on a solution which had been sealed under 1 atm of oxygen ($[O_2] = 1.5 \times 10^{-2}$ M)[25] and was kept in the dark at ambient temperature. First-order analysis of the absorption changes gave a rate constant, $k_{obs} = (3.5 \pm 1) \times 10^{-7}$ s$^{-1}$. The same product mixture, according to UV and TLC analysis, formed within 2 days when a solution of **2** was kept under 50 atm of oxygen in a steel cylinder. The main product was isolated in ca. 30% yield and identified as 7,7-dimethyl-3-formyl-4-(2-methylpropionyl)-6b,7a-dihydro-7*H*-cycloprop[*a*]acenaphthylene (**3**, Scheme I).

## Discussion

Cross-conjugated polyene 2,7-dihydro-2,2,7,7-tetramethylpyrene (**1**) and its valence isomers 2,2,7,7-tetramethyldicyclopropa[*a*,*g*]pyracene (*syn*-**2** and *anti*-**2**) form an unusual "inverse" photochromic system in which the thermodynamically more stable isomer **1** absorbs at longer wavelengths. Consideration of ring-strain contributions reveals why cross-conjugated polyene **1** is thermodynamically favored over its aromatic isomers **2**. Application of Benson's group increments[26] leads to the prediction that the thermal valence isomerization **2** → **1** is exothermic, $\Delta_{2\rightarrow1}H^{\ominus}(298\text{ K}) = -49$ kJ mol$^{-1}$. The two independent techniques of PAC and DSC gave an average value of −72 ± 10 kJ mol$^{-1}$ for the heat of reaction in solution. The free energies and enthalpies of the two geometric isomers of **2** are very nearly equal in apolar solvents; polar solvents stabilize the dipolar *syn* isomer relative to the *anti* isomer.

For the excited-state reactivity of this system, state-symmetry correlation[29] provides much more elaborate predictions than the simple "ground-state-forbidden ↔ excited-state-allowed" paradigm derived from the orbital symmetry conservation rules.[2] A state-symmetry correlation diagram for the lowest singlet and triplet states is shown in Figure 10. As in orbital-symmetry analysis, it is assumed that $C_s$ symmetry is retained throughout, i.e., that the plane of symmetry common to *syn*-**2**, *anti*-**2**, **1**, and **b** is retained along the reaction coordinate **2** → **b** → **1**. Electronic wave functions then classify as either symmetric (A′) or antisymmetric (A″) with respect to that element of symmetry.

(26) (a) Benson, S. W. *Thermochemical Kinetics*, 2nd ed.; Wiley: New York, 1976. (b) Standard heats of formation (g, 298 K) were calculated as $\Delta_fH^{\ominus}$(**1**) = 246 and $\Delta_fH^{\ominus}$(**2**) = 295 kJ mol$^{-1}$ based on the following assumptions. A value of +22 kJ mol$^{-1}$ was estimated for the missing increment $C(C_d)_2(C)_2$ on the basis of experimental data by Roth and Lennartz.[27] The ring strain contributions were obtained by adding twice the ring strain of acenaphthene (27 kJ mol$^{-1}$)[28] and of cyclopropane.[26a] Total strain in bicyclic hydrocarbons is usually close to the sum of the individual ring-strain contributions for the two fused rings.

(27) Lennartz, H.-W. Dissertation, Bochum, 1979.

(28) Boyd, R. H.; Christensen, R. L.; Pua, R. *J. Am. Chem. Soc.* **1965**, *87*, 3554.

(29) Salem, L. In *Electrons in Chemical Reactions: First Principles*; Wiley: New York, 1982. Klessinger, M.; Michl, J. In *Lichtabsorption und Photochemie organischer Moleküle*; VCH: Weinheim, 1989. Michl, J.; Bonačić-Koutecký, V. In *Electronic Aspects of Organic Photochemistry*; Wiley: New York, 1990.

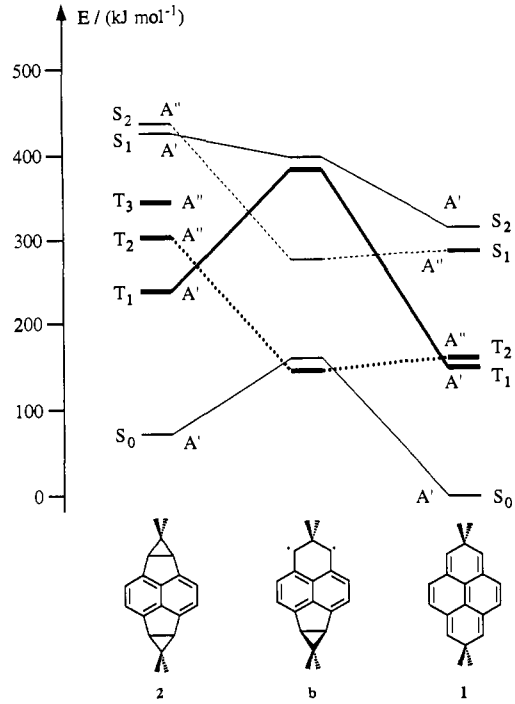


**Figure 10.** State-symmetry correlation diagram ($C_s$ point group). Bold lines connect triplet states, thin lines connect singlet states, dashed lines connect states of A″ symmetry, and solid lines connect states of A′ symmetry.

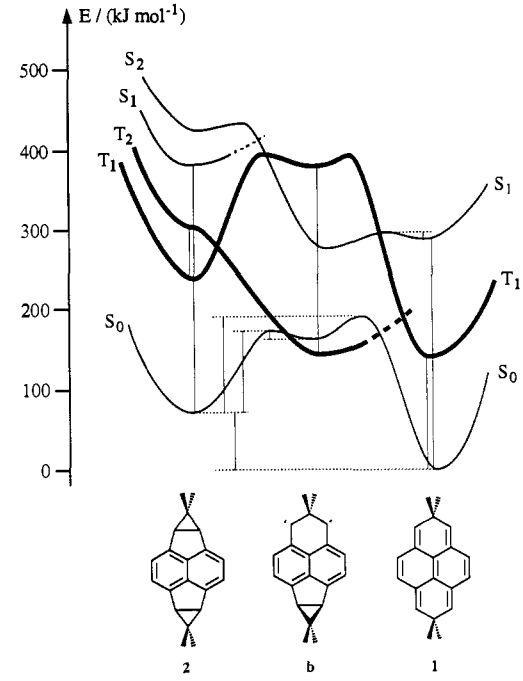


**Figure 11.** Potential surface diagram summarizing experimental data. Vertical lines mark experimental energy differences. Bold lines connect triplet states; thin lines connect singlet states.

Symmetry assignments of the lowest excited states of **1** and **2** are based on the spectroscopic data and calculations reported in the Results section. The symmetry assignments of the triplet states of **b** are the same as those established for related 1,8-naphthoquinodimethane biradicals.[5c,g-k]

Those for the singlet states of **b** are based on CNDO/S calculations with extensive CI (Table II). Note that adiabatic reactions from the lowest triplet state of both **1** and **2** to the triplet ground state of **b** and from the lowest excited singlet state of **2** to the lowest singlet state of **b** are forbidden. Nevertheless, the reaction appears to be feasible in the singlet manifold due to the presence of low-lying upper singlet states of **b** and the low-energy separation of the first from the second excited singlet state of **2**. Hence, the reactions from the lowest excited singlet states of **1** and **2** are expected to encounter only a small barrier. *Large, state-symmetry imposed barriers are expected for the formation of* $^3$**b** *from the lowest triplet states of* **1** *and particularly* **2**.

Figure 11 is a graphical summary of the experimental heats of reaction, electronic excitation energies, and kinetic activation energies determined in this work. Note the excellent agreement with the qualitative predictions derived from state-symmetry correlation, Figure 10. Experimental rate constants are collected in Table IV.

Biradical **b** was shown to be an intermediate on all thermal and photochemical paths connecting the three isomers **1**, *syn*-**2**, and *anti*-**2**. The thermal ring-flip reactions *syn*-**2** ⇄ *anti*-**2** and the valence isomerization **2** → **1** proceed entirely in the singlet manifold, and singlet biradical $^1$**b** is a short-lived ($\tau$ = 18 ps) reaction intermediate in these processes. Spontaneous intersystem crossing (ISC) to the triplet manifold is inefficient in thermal valence isomerization reactions, although surface crossing occurs along the reaction coordinate (biradical **b** has a triplet ground state). The photoinduced valence isomerization **1** ⇄ **2** also proceeds entirely in the singlet manifold at ambient temperature. Singlet biradical **b** is formed with near unit quantum yield from both isomers; it collapses predominantly by ring closure yielding **2** so that the photoinduced conversion **2** → **1** is an inefficient process. Entry to the triplet surface is provided by three pathways: triplet sensitization, photolysis at low temperature, and ISC catalyzed by diffusional encounter of singlet biradical $^1$**b** with triplet oxygen. At low temperature, $^3$**b** is formed in an adiabatic reaction from an upper triplet state of **2** that is populated by intersystem crossing from $S_1$. The triplet biradical is long-lived ($\tau$ = 660 $\mu$s at 25 °C in degassed acetonitrile) and is efficiently trapped by molecular oxygen.

We now comment on the experimental basis for these statements. Five questions will be addressed: (*i*) What is the evidence that singlet biradical $^1$**b** is an intermediate rather than a transition state? (ii) How can diffusional trapping of $^1$**b** by oxygen be efficient if its lifetime is only 18 ps? (iii) What reaction paths are followed after direct and sensitized excitation and, in particular, what is the evidence for the upper triplet state reaction of **2**? (iv) Why does the photostationary equilibrium shift from predominantly **2** at room temperature to exclusively **1** at 77 K? (v) Is the hypothesis of a single intermediate, $^1$**b**, in all photochemical and thermal reactions at room temperature consistent with all experimental results?

(i) Indirect evidence that $^1$**b** is a true reaction intermediate in the thermal ring-flip reaction of **2** comes from the kinetics of autoxidation in oxygenated solution. One possibility to be considered is that oxygen trapping arises from the interception of triplet biradicals $^3$**b** formed by *spontaneous* ISC during ring inversion. This is, however, not consistent with observation; $^3$**b** is trapped efficiently (>99.9%) in air-saturated solution. Therefore, increasing the oxygen pressure would not increase the rate of autoxidation if this mechanism were operative. In fact, the half-life of autoxidation of **2** decreases from about 1 mo under 1 atm to about a day under 50 atm of oxygen. This leaves oxygen trapping of singlet biradical $^1$**b** as the most obvious alternative. Since the ground state of **b** is a triplet state, we expect that *catalyzed* ISC converting $^1$**b** to $^3$**b** is efficient upon diffusive encounter of $^1$**b** with $^3O_2$.[30] Any $^3$**b** formed in this way will eventually be trapped by oxygen. According to this mechanism, a rate law for autoxidation is given by

(30) Saltiel, J.; Atwater, B. W. In *Advances in Photochemistry*; Volman, D. H., Hammond, G. S., Gollnik, K., Eds.; Wiley: New York, 1988; Vol. 14, pp 1–90.

$$-d[\mathbf{2}]/dt = (k_{a\rightarrow s} + k_{s\rightarrow a}) \times k_{cat}[O_2][\mathbf{2}]/(\tau^{-1} + k_{cat}[O_2]) \quad (4)$$

where $\tau$ is the lifetime of $^1\mathbf{b}$ in the absence of oxygen and $k_{cat}$ is the rate of catalyzed ISC which cannot exceed, but is likely[30] to approach, the rate of diffusion of oxygen in hexane, $k_{diff} \cong 3 \times 10^{10}$ $M^{-1}$ $s^{-1}$. Since the observed rate of autoxidation under 1 atm of oxygen, $k_{obs} = (3.5 \pm 1) \times 10^{-7}$ $s^{-1}$, is much slower than the rate of biradical formation, $k_{a\rightarrow s} + k_{s\rightarrow a} = (5.4 \pm 0.2) \times 10^{-5}$ $s^{-1}$, eq 4 may be simplified for the limiting case $k_{cat}[O_2] \ll \tau^{-1}$, eq 5. This simplified relation holds up to approximately 50 atm

$$-d[\mathbf{2}]/dt = (k_{a\rightarrow s} + k_{s\rightarrow a}) \times k_{cat}\tau[O_2][\mathbf{2}] = k_{obs}[\mathbf{2}] \quad (5)$$

of oxygen, as evidenced by the acceleration of autoxidation under oxygen pressure; at still higher pressures, one would expect saturation of the autoxidation rate when all singlet biradicals are intercepted. By inserting the known rates $k_{a\rightarrow s} + k_{s\rightarrow a}$ and $k_{obs}$ and assuming $k_{cat} \lesssim 3 \times 10^{10}$ $M^{-1}$ $s^{-1}$, the lifetime of $^1\mathbf{b}$ is estimated as $\tau \gtrsim 14$ ps. We recently used similar reasoning to estimate lifetimes of other singlet biradical intermediates.[5g,j,31] Here, for the first time, we are able to provide completely independent, direct evidence from picosecond flash photolysis: transient absorption attributed to $^1\mathbf{b}$, $\lambda_{max} \lesssim 345$ nm, was observed with a lifetime of $\tau = 18$ ps, in gratifying agreement with the estimate given above. Homoconjugation of the fused cyclopropane ring appears to be an important stabilizing factor in $^1\mathbf{b}$; the lifetime of the related biradical $^1\mathbf{c}$ derived from the naphthocyclopropane **4** was estimated to be less than 1 ps.[5g]

(ii) The lifetime of $^1\mathbf{b}$ estimated by assuming diffusional trapping of $^1\mathbf{b}$ by oxygen (eq 5) is fully consistent with that determined by picosecond flash photolysis. It may nevertheless seem counterintuitive that diffusional trapping can be efficient since the singlet biradical is so short-lived. In fact, diffusional trapping *is* quite inefficient; in aerated solution at room temperature, only about one-hundredth of the biradicals formed encounter oxygen during their lifetime. However, the ring-flip reaction of **2** is reversible and so biradical formation is repeated indefinitely until trapping occurs.

(iii) The variety of reaction paths connecting the three isomers in the closed system **1** ⇄ **2** is best followed in a graphical summary, Figure 11. Formation of biradical $^1\mathbf{b}$ is the predominant decay channel of **1** and **2** in the lowest excited singlet state $S_1$ at ambient temperature. The lifetime of $S_1(\mathbf{1})$ is 3 ps at room temperature, that of $S_1(\mathbf{2})$ is even shorter; fluorescence and ISC are too slow to compete effectively. At 77 K, the small activation barriers opposing the formation of $^1\mathbf{b}$ from $S_1(\mathbf{1})$ and $S_1(\mathbf{2})$ are sufficient to quench these reactions. On the other hand, no significant barrier appears to impede the ring cleavage of **2** in the triplet manifold; spontaneous ISC of **2** after excitation at 77 K yields $^3\mathbf{b}$ within <100 ns. Sensitization experiments with triplet sensitizers of different energy have shown that this reaction occurs exclusively from an upper triplet state of **2**, as predicted by state-symmetry analysis. The lowest triplet state $T_1(\mathbf{2})$, if formed by energy transfer from a sensitizer with low triplet energy, is long lived and nonreactive. Since $T_1(\mathbf{2})$ is *not* observed by flash photolysis when a high-energy sensitizer (benzophenone) is used or when spontaneous ISC occurs at low temperature, we conclude that adiabatic ring fission of $T_2(\mathbf{2})$ yielding $^3\mathbf{b}$ is much faster than the internal conversion $T_2(\mathbf{2}) \rightarrow T_1(\mathbf{2})$.

(iv) At 77 K, photoisomerization is one-way, **2** → **1**. This is surprising because the reverse reaction is much more efficient at room temperature (cf. photostationary equilibrium, Figure 1). This reversal of photoreactivity is due to a change in the reaction mechanism with temperature. At ambient temperature, the reaction proceeds entirely in the singlet manifold. At 77 K, $^3\mathbf{b}$ is formed by spontaneous ISC of $S_1(\mathbf{2})$ followed by adiabatic ring fission of $T_2(\mathbf{2})$. Excitation of persistent biradical $^3\mathbf{b}$ with a second photon then gives **1** which is stable to irradiation at 77 K. We assume that excitation of $^3\mathbf{b}$ yields $T_1(\mathbf{1})$ in an adiabatic reaction, by analogy to the closely related adiabatic cyclization of excited triplet 1,8-naphthoquinodimethane to triplet acenaphthene.[5k]

(v) If all photochemical (**1** ⇄ **2**) and thermal (**2** → **1**, *anti*-**2** ⇄ *syn*-**2**) reactions proceed *via* the same singlet biradical intermediate $^1\mathbf{b}$, then how can the photochemical quantum yield $\phi_{2\rightarrow 1} = 0.05$ be reconciled with the $10^4$-fold preference of $^1\mathbf{b}$ to cyclize to **2** rather than to cleave the second cyclopropane ring yielding **1**? Singlet biradical $^1\mathbf{b}$ is thermally excited when formed from $S_1(\mathbf{1})$ or $S_1(\mathbf{2})$, and it is reasonable to expect that the process $^1\mathbf{b} \rightarrow \mathbf{1}$ is sufficiently fast to compete with the thermal relaxation of hot $^1\mathbf{b}$. In fact, the picosecond flash photolysis experiments provide some evidence for such a hot ground-state reaction: the formation of **1** following pulsed excitation of **2** appears to be complete within a few picoseconds whereas the lifetime of $^1\mathbf{b}$ is 18 ps. It is worth noting explicitly that $^1\mathbf{b}$ preferentially yields the thermodynamically less stable isomers of **2**. A barrier to cyclopropane ring closure, $^1\mathbf{b} \rightarrow \mathbf{2}$, can be estimated at a mere 1.5 kJ $mol^{-1}$ from the lifetime of $^1\mathbf{b}$ by assuming a "normal" *A* factor of about $10^{13}$ $s^{-1}$ for this reaction. Based on activation parameters for equilibration of isomers of **2** and for the conversion of **2** to **1** (Table IV), cleavage of the second cyclopropane ring requires a substantial activation energy of 20 ± 3 kJ $mol^{-1}$.

Aspects regarding a possible application of the photochromic system **1** ⇄ **2** have not been of concern in this work, and we have made no attempts to determine fatigue in repeated cycles. The only side reactions we noticed are due to oxygen trapping of biradical intermediates, and this is very inefficient without triplet sensitizers except under high oxygen pressure. Clearly, a more efficient synthetic approach allowing for the introduction of auxochromic substituents would be a prerequisite for conceivable applications.

We have shown that biradical **b** is an intermediate in all thermal and photochemical transformations **1** ⇄ **2**. At room temperature and above, all reactions proceed in the singlet manifold; ISC occurs only if singlet biradical $^1\mathbf{b}$ encounters molecular oxygen during its lifetime of 18 ps. At 77 K, spontaneous ISC of **2** dominates the photoreactions. The reaction from $^3\mathbf{2}$ to $^3\mathbf{b}$ starts from an upper excited triplet state, as predicted by state-symmetry analysis.

## Experimental Section

**Optical Spectra.** Absorption spectra were recorded on a Beckman UV 5240. A thermostated quartz dewar was used to record low-temperature spectra down to 77 K. Solutions of **1** and **2** in EPA were immersed in liquid nitrogen to determine fluorescence spectra on a Spex Fluorolog 2 (Model 111 C) equipped with a red-sensitive R666 S photomultiplier tube. Excitation spectra were corrected (up to 590 nm) using a Rhodamine 6 G quantum counter; emission spectra were corrected in the range of 250–850 nm using scale factors determined with a calibrated, 45-W tungsten filament source (Optronic Laboratories, Model 245C, L-190). The fluorescence spectrum of a sample of **1** isolated in an argon matrix by vacuum codeposition (1:1000) on a CsI window held at 12 K was also determined on the same instrument. For phosphorescence measurements, a pulsed lamp accessory (Model 1934 C) was available.

**Nanosecond Kinetic and Spectrographic Flash Photolysis.** Pulses of ca. 20-ns duration from a frequency-doubled (532 nm) or -tripled (355 nm) Nd–glass laser and from a XeF excimer laser (351 nm) or of 20-μs pulse width from a conventional electric discharge were used for excitation. The detection system allowed for the capture of transient kinetics (at a given wavelength) or of the transient spectrum (at a given time delay after excitation) in digital form with nanosecond time resolution. Kinetic and spectrographic data were processed and analyzed by computer. Details of the experimental setup have been described.[32]

**Picosecond Spectrographic (Pump–Probe) Flash Photolysis.** The laser used is based on a dual cavity excimer laser (Lambda Physik, EMG 150) of which one cavity is used for pumping a cascade of dye lasers (Laser Laboratorium Göttingen). The heart of the dye laser setup is a distributed

(31) Adam, W.; Platsch, H.; Wirz, J. *J. Am. Chem. Soc.* **1989**, *111*, 6896.

(32) (a) Wirz, J. *Pure Appl. Chem.* **1984**, *56*, 1289. (b) Leyva, E.; Platz, M. S.; Persy, G.; Wirz, J. *J. Am. Chem. Soc.* **1986**, *108*, 3783. (c) Gerber, S.; Wirz, J. *EPA Newsletter* **1989**, *36*, 19.

feedback dye laser that gives green pulses at 496 nm of 0.5-ps duration. Its output is amplified, frequency doubled, and used to seed the second, synchronously pumped cavity of the excimer laser. A 0.5-ps pulse at 248 nm with a typical energy of ≈3.5 mJ (4% standard deviation) on an area of about 1 × 1.5 $cm^2$ is obtained. The 496-nm beam left after frequency doubling has an energy of about 180 μJ (4% standard deviation) and is used for continuum generation.

The pump-and-probe setup was similar to that described by Ernsting and Kaschke.[33] The continuum for probing is produced by focusing the 496-nm laser beam into a 5-mm quartz cell with a quartz lens of 20-mm focal length placed at a distance of 18.8 cm from the cell surface. The cell was filled with a 1:1 mixture of $H_2O$ and $D_2O$. This generates a continuum of ca. 0.5-ps duration that extends from 310 to 700 nm. The continuum is collected by a spherical mirror, and the central part containing residual laser light is blocked. A 50% beam splitter divides the continuum light into a reference and a probe beam. Both beams pass the sample cell, spectral filters, and a Glan polarizer that is set at the magic angle relative to the polarization of the pump beam. Finally, the beams are focused onto the slit of a 0.275-m spectrograph, covering a spectral range of 400 nm. A double diode array (512 diodes each, Princeton Instruments DDA-512) is used for recording the spectra of the probe and the reference beam simultaneously.

The 248-nm beam, which is used for pumping, is collimated by a quartz lens ($f$ = 3 m). Its central part is selected by a variable aperture and directed through a variable delay line of up to 2 × 30-cm length providing delay times of up to 2 ns. Then the beam is loosely focused by a quartz lens ($f$ = 50 cm) and superimposed on the spot where the probe continuum hits the sample. With this setup, the sample is pumped by about 1 mJ of 248-nm light on an area of 4 $mm^2$, corresponding to 3 photons per $Å^2$.

The sample cell is a quartz cell with a path length of 2 mm. A gear pump is used for continuously circulating the sample through the cell. Typically, 400 spectra are accumulated at a repetition rate of 12 Hz for each delay setting.

The effective time resolution of our setup was defined by the cross correlation of the pump and continuum pulses. Strong absorption of the probe pulse was observed even in "transparent" samples when it passed the sample at the same time as the pump pulse. This is attributed to two-color, two-photon absorption by the solvent.[33] At a given wavelength of observation (390 nm), the absorption of the probe pulse exhibited a Gaussian time profile with a full width at half-maximum (fwhm) of 1.2 ps. Assuming that both pulses had the same shape and pulse width, we concluded that their individual fwhm is about 0.8 ps at the sample. The same phenomenon could also be used to measure the group velocity distribution of the continuum pulse by observing the shift of the maximum of the two-photon absorption spectrum as a function of time. In the range of 350–440 nm, we found a linear relationship with a slope of about 40 nm/ps.

**Analysis of Picosecond Spectra.** A series of spectra was recorded at different delays with respect to the pump flash. These spectra were assembled row-wise in a data matrix $\mathbf{Y}(m \times w)$ and decomposed into a product of three matrices $\mathbf{U}(m \times r)$, $\mathbf{S}(r \times r)$, $\mathbf{V}(r \times w)$ by singular value decomposition,[34]

$$\mathbf{Y} = \mathbf{USV}$$

where $m$ is the number of spectra taken, $w$ is the number of data points per spectrum, and $r$ is the rank of matrix **Y**. The rows of **V** are the eigenspectra. Each element $u_{ij}$ of **U** gives the weight of the $j$th eigenspectrum in the $i$th observed spectrum ($i$th row in **Y**). The elements of diagonal matrix **S** indicate the total importance of each eigenspectrum. **U**, **S**, and **V** are completely abstract and have no physical meaning. The matrices **U**, **S**, and **V** can be reduced to $\mathbf{U}'(n \times n)$, $\mathbf{S}'(n \times n)$, and $\mathbf{V}'(n \times n)$ taking only $n$ significant components into account, thus eliminating experimental noise. The size of $n$ is determined by considering the diagonal elements of **S** that usually lie below the noise level except for the two or three largest values. This is tantamount to saying that a series of spectra taken at different delay times is usually composed of only two or three components with linearly independent spectra. Multiplication of the set of reduced matrices yields the matrix $\mathbf{Y}' = \mathbf{U}'\mathbf{S}'\mathbf{V}'$ that contains the relevant spectral information. The spectra displayed in Figures 7–9 are in fact rows of reduced data matrices **Y**′.

Since the observed spectra can be reproduced by linear combination of the eigenspectra, the weights of the eigenspectra obey the same kinetics as the real components. This was used in the global kinetic analysis of the data: a (multi)exponential function was fitted to the columns of matrix product **U**′**S**′ such that the sum of squares of the errors was minimized.[35a] It has been shown that this procedure leads to essentially the same rate constants as those fitting the original set of spectra but dramatically decreases the time needed for computation.[35b]

**Photoacoustic Calorimetry.** The front face irradiation cell and algorithm used for data analysis were those described by Caldwell, Melton, and co-workers.[36] Excitation pulses from a XeF excimer laser of 25-ns pulse width were attenuated to an energy of ca. 1 mJ per pulse. A dielectric mirror (>99.9% reflection at 351 nm, 90° incidence angle) was used to reduce the background signal. The cell thickness of 0.2 mm was fixed with a Teflon spacer. The signal of a 1 MHz contact transducer (Panametrics, A103) was fed into a 200-Ω input on a transient digitizer (Tektronix 7912AD). 2-Hydroxybenzophenone in acetonitrile was used as a calibration standard for the system response (T wave). The absorbances of the reference and sample solutions were adjusted to the same value around 0.5 to within 0.001 absorbance unit in a 1-mm cell. A flow cell was used to ensure exposure of fresh solutions for each shot. Eight traces were collected and averaged for each measurement; shot-to-shot variations in the excitation pulse energy were monitored with a pyroelectric energy meter (Laser Precision Co., Rj-7620 energy meter, RjP-734 probe head) and were usually within ±2%. Each shot was normalized to correct for these small variations. Four independent measurements of both sample and reference were analyzed.

**Autoxidation of 2.** The syntheses of dihydropyrene **1** and its valence isomers *syn*-**2** and *anti*-**2** have been described.[4] A 1:1 mixture of *syn*-**2** and *anti*-**2** (20 mg) in $CCl_4$ (5 mL) was kept under ca. 50 atm of oxygen in a steel cylinder for 48 h at ambient temperature (ca. 20 °C). Thin layer chromatography on silica with $CHCl_3$ as an eluent showed that the product mixture was free of starting material *syn*-**2** or *anti*-**2** and contained at least six components. The major product ($R_f$ = 0.29, sticky oil, ca. 8 mg) was "distilled" under vacuum and identified as 7,7-dimethyl-3-formyl-4-(2-methylpropionyl)-6b,7a-dihydro-7*H*-cycloprop[*a*]acenaphthylene (**3**) on the basis of the following spectral data. MS: 292 ($M^+$, 5.1), 277 (42), 275 (36), 250 (20), 249 (100), 235 (24), 234 (72), 222 (11), 221 (43), 178 (39), 177 (15), 176 (14), 152 (11), 151 (12), 43 (28), 41 (10). IR (neat): 2720 (m), 1690 $cm^{-1}$ (br, vs). $^1H$ NMR ($CDCl_3$, TMS, 400 MHz): δ 0.47 (3H, s, $C_7$-$CH_3$), 1.21$_5$ (3H, d, $J$ = 7 Hz, [CH]$CH_3$), 1.24 (3H, d, $J$ = 7 Hz, [CH]$CH_3$), 1.37 (3H, s, $C_7$-$CH_3$), 2.96 (1H, d, $J$ = 5 Hz, H-6b or H-7a), 3.01 (1H, d, $J$ = 5 Hz, H-6b or H-7a), 3.22 (1H, sept, $J$ = 7 Hz, $[CH_3]_2CH$), 7.41 (1H, d, $J$ = 7 Hz, H-1 or H-6), 7.48 (1H, d, $J$ = 7 Hz, H-1 or H-6), 7.65 (1H, d, $J$ = 7 Hz, H-2 or H-5), 7.97 (1H, d, $J$ = 7 Hz, H-2 or H-5), 10.04 (1H, s, CHO).

**Acknowledgment.** This work was supported by the Swiss National Science Foundation. Financial support was obtained from the Fonds zur Förderung von Lehre und Forschung and the Ciba-Geigy Jubiläumsstiftung. H.P. thanks the Deutsche Forschungsgemeinschaft for a postdoctoral research fellowship. We are grateful to Prof. J. Streith and his co-workers Drs. P. Goursot and H. Strub, Mulhouse, for their help in performing the DSC measurements; to Profs. S. Braslavsky, MPI Mülheim, and R. A. Caldwell and L. A. Melton, UT Dallas, for teaching us the art of PAC; to Dr. B. Dick, MPI Göttingen, for CNDO/S calculations of **b**; and to Dr. N. Ernsting, Göttingen, for advice concerning the picosecond detection system.

(33) Ernsting, N. P.; Kaschke, M. *Rev. Sci. Instrum.* **1991**, *62*, 600.
(34) Malinowski, E. R. In *Factor Analysis in Chemistry*, 2nd ed.; Wiley: New York, 1991.
(35) (a) Gampp, H.; Maeder, M.; Zuberbühler, A. D. *Talanta* **1980**, *27*, 1037. (b) Gampp, H.; Maeder, M.; Meyer, C. J.; Zuberbühler, A. D. *Talanta* **1985**, *32*, 95.
(36) Ni, T.; Caldwell, R. A.; Melton, L. A. *J. Am. Chem. Soc.* **1989**, *111*, 457. Melton, L. A.; Ni, T.; Lu, Q. *Rev. Sci. Instrum.* **1989**, *60*, 3217.